Nexus
Research article

Structural coloring of solar photovoltaics with quasi-ordered photonic pigments

Zhenpeng Li, Tao Ma, Yuning Chen, Sinan Li, Yanjun Dai, Dongshi Zhang, Hongxing Yang, and Jinyue Yan
*Correspondence: tao.ma@sjtu.edu.cn

IN BRIEF

Inspired by nature, Li et al. develop colorful and whitish solar panels using quasi-ordered photonic pigments that selectively scatter visible light. This scalable technology yields diverse non-iridescent, natural hues for solar panels while maintaining high efficiency, showing great potential to enable seamless building integration for a more sustainable built environment.

Nexus
Research article

Structural coloring of solar photovoltaics with quasi-ordered photonic pigments

Zhenpeng Li,[1,5] Tao Ma,[1,6,*] Yuning Chen,[1] Sinan Li,[1] Yanjun Dai,[1] Dongshi Zhang,[2] Hongxing Yang,[2] and Jinyue Yan[3,4]

[1]Engineering Research Centre for Solar Energy and Refrigeration of Ministry of Education, School of Mechanical Engineering, Shanghai Jiao Tong University, Shanghai 200240, China

[2]Shanghai Key Laboratory of Materials Laser Processing and Modification, School of Materials Science and Engineering, Shanghai Jiao Tong University, Shanghai 200240, China

[3]Department of Building Environment and Energy Engineering, The Hong Kong Polytechnic University, Hong Kong, China

[4]International Centre of Urban Energy Nexus (UEX), The Hong Kong Polytechnic University, Hong Kong, China

[5]Present address: Department of Civil and Environmental Engineering, Princeton University, Princeton, NJ 08540, USA

[6]Lead contact

*Correspondence: tao.ma@sjtu.edu.cn

https://doi.org/10.1016/j.ynexs.2025.100101

BROADER CONTEXT

Integrating solar panels into buildings can greatly boost the use of renewable energy. However, their dark and unattractive appearance often limits acceptance by architects and homeowners. Adding color to solar panels is not straightforward, as it requires balancing light absorption for power generation with light reflection for color. By combining insights from physics, material science, and engineering, this work proposes a bird-feather-like optical design for solar panels, which separates visible light scattering from light absorption. More importantly, this work demonstrates that, by using eco-friendly materials and scalable fabrication techniques, such optical design can be easily integrated with solar panel production processes, enabling naturally colorful solar panels that retain high efficiency. By blending into building surfaces without drawing attention, this technology could accelerate the adoption of solar energy in the built environment and support the transition to a more sustainable future.

ABSTRACT

Solar photovoltaic (PV) modules that are non-black but visually appealing can enhance their integration with roofs, facades, and vehicles. Inspired by the blue feather combing a keratin-air network with black melanin to create structural color, we herein demonstrate the coloring of PV modules by placing quasi-ordered photonic pigments atop solar cells. These pigments, composed exclusively of silica microspheres and polyacrylates, enable selective and diffuse reflection of visible light while negligible absorption of solar radiation. When incorporated into the encapsulation layers of industrial-grade silicon solar cells, they yield PV modules with non-iridescent and vibrant colors reminiscent of natural hues, such as sky blue and grayish-white. The colored PV modules exhibit power conversion efficiencies ranging from 19.4% to 21.2%, representing more than a 50% improvement compared with conventional pigments. When applied to building facades, they can boost the power generation potential of building-integrated PVs by 33%–54% across densely populated regions worldwide.

INTRODUCTION

Buildings currently account for over 30% of global energy consumption and CO_2 emissions.[1] Although passive technologies, such as radiative cooling,[2,3] smart windows,[4] and thermal insulations,[5,6] effectively reduce energy intensity, the rising global energy demand in buildings necessitates on-site renewable generation.[7] Solar photovoltaics (PV) offer a promising solution, but its widespread deployment in built environments is constrained by limited land availability. This limitation motivates the development of integrated PV technologies, intending to incorporate PV modules into building envelopes (building-integrated PV [BIPV] systems), vehicles (VIPV), as well as infrastructures such as noise barriers and road fences.[8–10] However, the limited esthetic appeal and the incongruity with the urban landscape of conventional PV modules greatly hinder that.[11,12]

PV modules are typically black due to their highly light-absorptive nature for achieving high power conversion efficiency (PCE). To modify them with colored or white appearance while preserving high PCE, a coloring layer that reflects (or emits) a part of visible light ($\lambda \sim 400$–700 nm) while being transparent for other sunlight is required (Note S1).[13–15] Despite many efforts, the coloring material that meets such optical properties while being cost-effective in PV colorization process remains a significant challenge.[16] For example, multilayer dielectric thin films such as Bragg reflectors, capable of selectively reflecting visible light, have demonstrated potential for colorizing PV modules with less than 10% relative PCE loss.[17–19] However, their inherent iridescence, glare, and higher manufacturing costs may limit scalability and practical use.[20–22] Alternative materials, such as silver plasmonic nanoparticles,[23] cholesteric liquid crystals,[24] and photoluminescent quantum dots,[25] also face challenges related to scalability and color performance.

Nature offers various color strategies to learn, especially those using special micro-nanostructures to create structural color without dyes or pigments.[26] For example, bird feathers realize blue color by their spongy layer composed of β-keratin and air, combined with an underlying melanin layer (Figure 1A).[27,28] The spongy layer, characterized by a nanoporous structure with short-range order while long-range disorder, selectively scatters short-wavelength light. Since the light transmitted is subsequently absorbed by melanin granules beneath, a non-iridescent vibrant blue color is displayed, which can also be tuned by the thickness and structure of the spongy layer. Inspired by this natural mechanism, in this work we propose an optical design for colored PV modules. As depicted in Figures 1A and 1B, this design integrates a transparent glass cover (analogous to the cortex layer), a structural coloring layer with quasi-ordered photonic structures (analogous to the spongy layer), and high-efficiency black solar cells (resembling melanin granules). Although colored PV modules and bird feathers appear totally unrelated, in this context they share nearly identical optical structures.

A distinguishing feature of this design is the decoupling of partial scattering and residual visible light absorption. This not only ensures that the combined effect still achieves a natural color appearance comparable with traditional pigments but also strategically leverages the

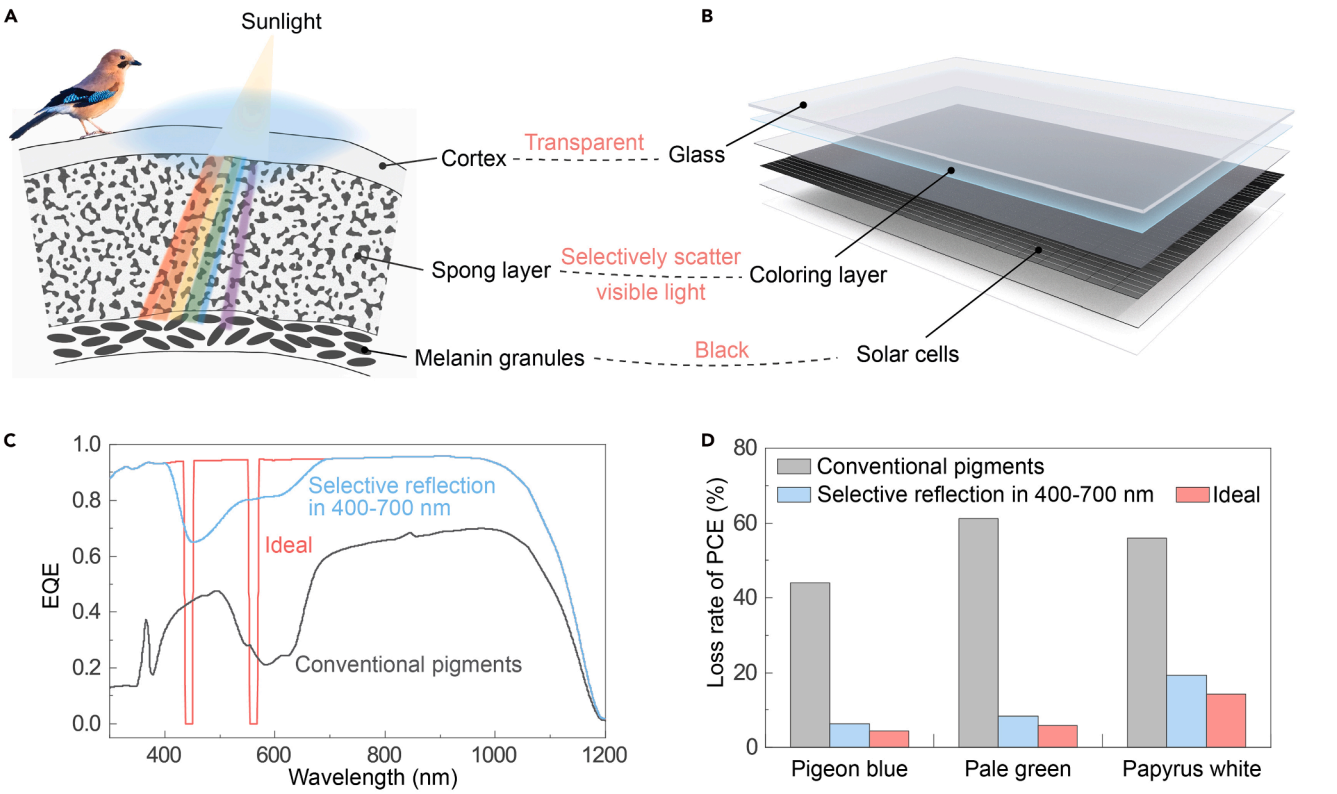

Figure 1. Bio-inspired optical design of the colored PV module

(A and B) Schematic showing (A) the cross-sectional structure of blue feather barbs of the Eurasian jay[27] and (B) the colored PV module. With a coloring layer involving quasi-ordered photonic structures for selective scattering of visible light, the colored PV module exhibits identical optical structures with the blue bird feather.

(C) The simulated external quantum efficiency (EQE) of colored PV modules made by coloring layers with different optical properties. They all show a pigeon blue color (RAL 5014).

(D) The simulated loss rate of PCE when using different coloring layers for the colorization of PV modules.

intrinsic requirement of solar cells to be highly absorptive for optimal power generation. In contrast, conventional pigments simultaneously scatter and absorb light.[29] If they were used to colorize PV modules, the external quantum efficiency (EQE) and PCE would be significantly reduced (Figures 1C and 1D; see details in Note S2). This explains why colored PV modules using conventional pigments are commonly dark and have PCEs typically below 15%.[30–32] In contrast, when the coloring layer has no absorption but just selectively reflects visible light, the PCE loss rate is less than 10% for a pigeon blue coloration and is still below 20% in the case of papyrus white coloration (Figure 1D; Table S1). In this regard, some other well-developed structural color materials, such as multilayer films or optical metasurfaces,[33] can also achieve similar functionality. However, their distinctive color effects are not well suited for the esthetic and practical requirements of most integrated PV applications. As comparison, a quasi-ordered photonic structure as found in the spongy layer of blue feathers, is particularly favored as it enables more diffuse reflection,[34,35] promising a structurally coloring appearance similar to most daily objects while avoiding iridescence and glare effects.

To validate this design and ensure that the quasi-ordered photonic structure can be seamlessly integrated into PV modules without relying on high-cost or scalability-limited methods, in this work we further develop a distinctive type of photonic pigment, i.e., silica-polyacrylate structural color (SPSC) pigment. The pigment features a stable quasi-ordered photonic structure assembled from colloidal silica microspheres, with easy-adjustable structural coloration and high transparency to solar radiation. We then demonstrate that SPSC pigments enable originally black PV modules to achieve variously colored or white coloration, with significantly lower PCE losses compared with conventional pigments. Finally, we underscore the potential of these highly efficient and visually appealing PV modules to boost solar power generation in densely populated urban regions worldwide.

RESULTS

SPSC pigments

Employing a structural coloring layer poses great challenges in the fabrication scale and cost. In contrast, pigment color can be easily applied onto PV modules using screen printing or inkjet printing, which is a commonly used coloring technique in industry.[36–38] Inspired by that, we propose to first process structural color materials into pigments and then apply them for coloring PV modules. To fabricate such quasi-ordered photonic pigments for structurally coloring PV modules, here we have developed a preparation strategy different from reported methods.[39–41] We exploited the densely packed silica microspheres as the precursors for creating structural color (Figure S2). By infiltrating acrylates and ultraviolet (UV) curing them to stabilize the dense-packing structure, we then prepared the pigment particles by mechanical grinding (refer to methods and Figure S3 for details). This significantly simplifies the preparation process and facilitates its scaling up.

As shown in Figure 2A, these SPSC pigments particles have random shapes and various sizes since they are made by a mechanical grinding process. By using a 150-mesh screen for sorting, the pigment particles primarily range from tens to 100 μm. Higher magnification images show that each pigment particle comprises densely packed microspheres of nearly identical size (Figure 2A, right). Despite the non-flat pigment surface resulting from the mechanical grinding process, most microspheres are arranged regularly, with polyacrylates filling the gap and adhering to each other. As a typical feature of

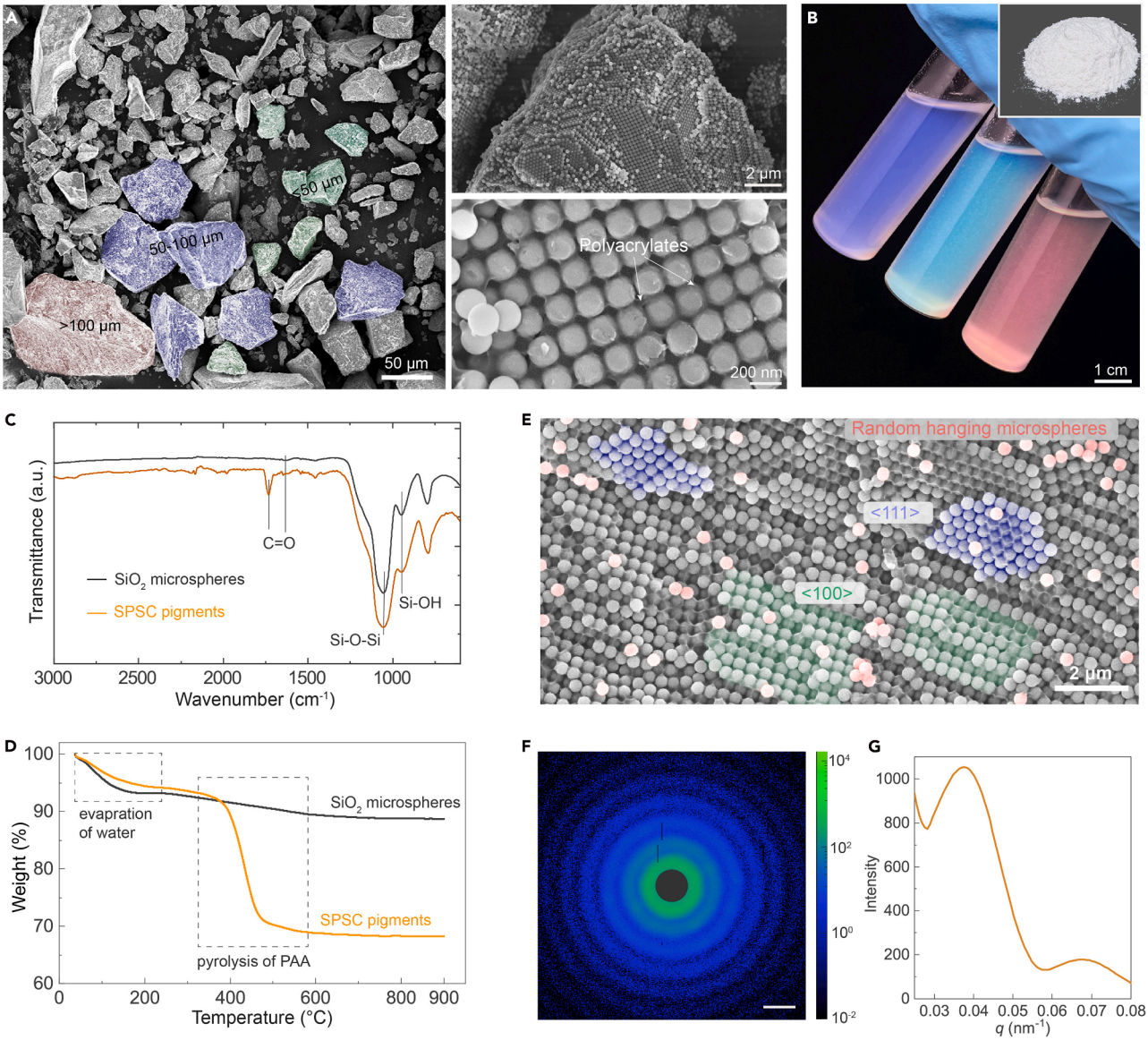

Figure 2. Characterization of SPSC pigments

(A) SEM images of the SPSC pigments at 200×, 5k×, and 50k× magnification, respectively. The pigment particles have various shapes and sizes, formed by regularly arranged monodispersed silica microspheres and polyacrylate jointing the microspheres.

(B) Photograph of the SPSC pigments dispersed in clear resins. Inset: dry pigment powder in white.

(C and D) (C) Fourier transform infrared spectroscopy and (D) thermogravimetric analysis of the SPSC pigments, with comparison of pure silica microspheres.

(E) SEM image of a pigment surface.

(F and G) (F) Small-angle X-ray scattering pattern and (G) azimuthal X-ray intensity as a function of scatter vector (q), obtained from a piece of film made by the SPSC pigments with blue color. Scale bar, 0.05 nm^{-1}.

non-absorbing structural color pigments, SPSC pigments appear entirely white as dry powders in the air. However, when dispersed in a clear liquid such as water, ethanol, or acrylate to suppress random multiple scattering of light, the color effect becomes immediately apparent (Figure 2B). Besides, they exhibit vivid reflection colors against a black background, but appear colorless and translucent in transmitted light, demonstrating very high transparency (Figure S4).

Polyacrylates were utilized to stabilize the assembled structure of silica microspheres, enabling the pigments to be processed with a mechanical grinding method and thus promoting the scalability of production. Without this stabilization, the orderly arrangement of microspheres could be easily disrupted (Figure S5). Fourier transform infrared spectroscopy (FTIR) manifests the abundance of silicon hydroxyl groups on silica microspheres and carboxyl groups from the infiltrated acrylates (Figure 2C). These groups can establish hydrogen bond interactions, which elucidates why the acrylate resin and silica microspheres can form a stable structure post UV curing.[34] According to thermogravimetric analysis, about 20% of the weight of SPSC pigments was lost at approximately 400°C, which is attributed to the pyrolysis of polyacrylates (Figure 2D). This indicates that ~30% of the pigment volume is occupied by polyacrylates, which has essentially filled the interstices among densely packed silica microspheres.

The assembly structure of colloidal microspheres plays a pivotal role in determining optical properties. In the case of SPSC pigments, silica microspheres are typically arranged in a regular pattern, similar to colloidal photonic crystals,[42] while different crystal planes are randomly exposed, such as <111> and <100> planes of a

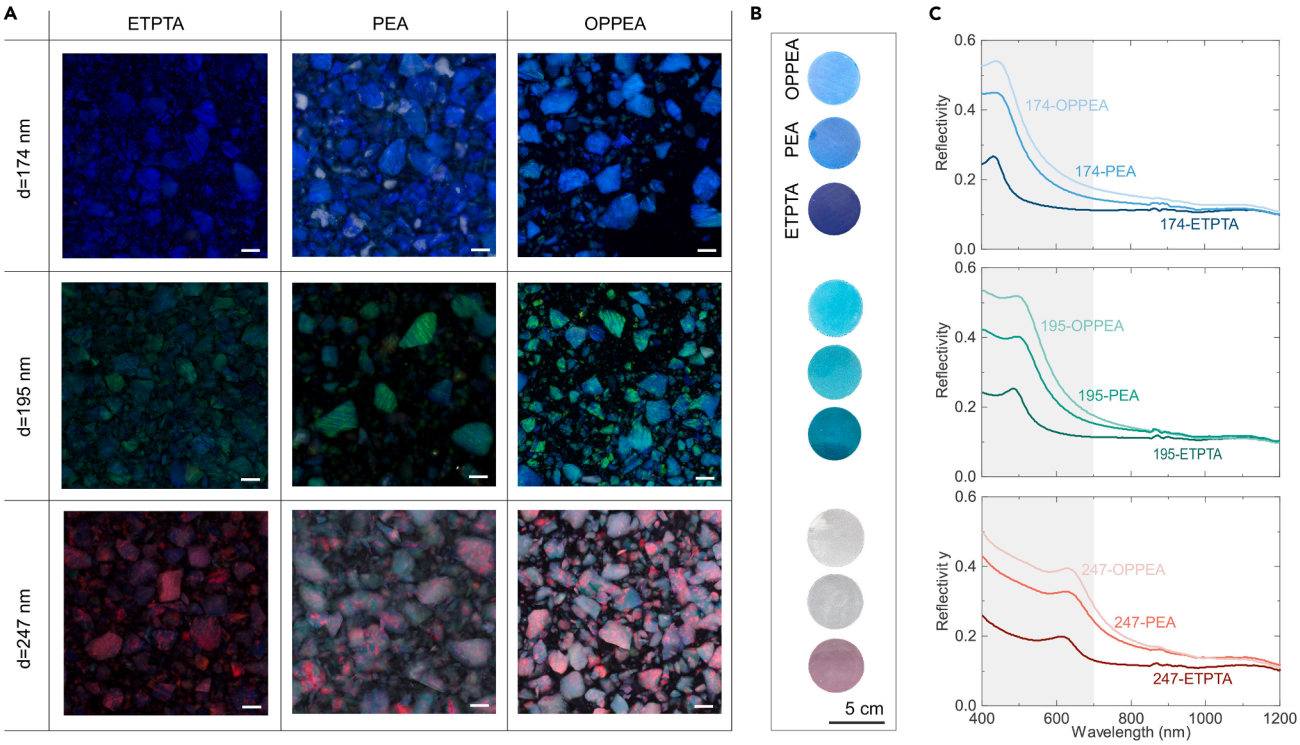

Figure 3. Modifying structural color by microsphere size and refractive index of acrylates

(A) Dark-field optical microscopy images of the SPSC pigments made by silica microspheres of different diameters *d* and different types of acrylates, including ethoxylated trimethylolpropane triacrylate (ETPTA), 2-phenoxyethyl acrylate (PEA), and O-phenylphenoxyethyl acrylate (OPPEA). The pigments are observed when impregnated within ETPTA. Scale bars, 100 μm.

(B and C) (B) Photographs of the films composed of different SPSC pigments and their (C) spectral reflectivity, showing different reflection intensity and different characteristic reflection peaks.

face-centered cubic structure (Figure 2E). Additionally, there are numerous hollows and hanging microspheres randomly distributed on the surface. These factors make the overall photonic structure of the SPSC pigments unclear through microscopic observation. For this reason, we used small-angle X-ray scattering (SAXS) to quantify the average structural correlations of SPSC pigments when they are dispersed in coloring coatings.[43,44] The measured 2D SAXS data of a blue film containing the pigments exhibits a ring-like pattern with only minor variations in different directions (Figure 2F). This suggests that the structure is nearly isotropic and quasi-ordered, similar to colloidal photonic glass and the photonic structure present in blue bird feathers.[44,45] The azimuthal-averaged scattering intensity as a function of scattering vector (q) is plotted in Figures 2G and S6, with the first main peak located at $q_{peak} \approx 0.037$ nm^{-1}. Given that the full-width at half-maximum of this peak (Δq) is about 0.019 nm^{-1}, the spatial order range is estimated to be $\xi = 2\pi/\Delta q \approx 331$ nm, which is only about two times the diameter of silica microspheres. The disruption of long-range order can restrain the angular dependence of structural color.[46]

Modification of structural color

For photonic structures self-assembled by monodisperse microspheres, when the assembly protocol remains identical, the wavelength of the reflection peak λ_{peak} is determined by the microsphere diameter d and effective refractive index n_{eff}, i.e.,[47]

$$\lambda_{Peak} = k \cdot n_{eff} d$$

where k is a coefficient determined by the assembly structure. Additionally, the reflection intensity is influenced by the contrast in refractive index between microspheres and the matrix. Therefore, the optical properties and structural color of SPSC pigments can be easily adjusted. Various types of structural color pigments were fabricated using silica microspheres with different diameters (Figure S7) and different acrylates with distinct refractive indices, namely ethoxylated trimethylolpropane triacrylate (ETPTA) (n = 1.471), 2-phenoxyethyl acrylate (n = 1.515), and O-phenylphenoxyethyl acrylate (OPPEA) (n = 1.577). As dry powders, all SPSC pigments derived from diverse materials appear colorless and are thus indistinguishable (Figure S8). However, when impregnated in a liquid medium, they display varying color effects under dark-field optical microscopy, indicating the selective scattering of different visible light (Figures 3A and S9). Increasing microsphere size leads to color change from blue to red, while transitioning from ETPTA to OPPEA leads to a tendency for the color to become brighter and less saturated.

Subsequently, we mixed these SPSC pigments with polyurethane acrylates and UV-initiating agents, producing UV-curable structural color resins (Figure S10). Figure 3B presents the films (~300 μm thick) cured by the resins containing different pigments, showing different colors against a black background. Except for the pigments made of ETPTA, the displayed colors remain almost unchanged when the observed angle increases (Figure S11). The reflectance spectrum presented in Figure 3C clearly indicates that λ_{peak} increases with d, thereby leading to different color hues. Using acrylates with a higher refractive index slightly enlarges λ_{peak}, while significantly enhancing reflection intensity and thus rendering the color brighter and less saturated. It is noteworthy that, for microspheres with d of 247 nm, the resulting color appears so unsaturated that it closely resembles white. Therefore, the SPSC pigments could achieve a wide range of colors within the blue and green color families by modifying the microsphere size, acrylate materials, and pigment usage. Gray and white are also realizable at a low near-infrared (NIR) reflectivity, but an angle-independent red color is restricted, which is an intrinsic limitation of quasi-ordered photonic materials.[47,48]

Colored PV modules

The SPSC pigments exhibit a predominant reflection of visible light and a rapid decrease in reflectivity toward NIR wavelengths. Besides, both

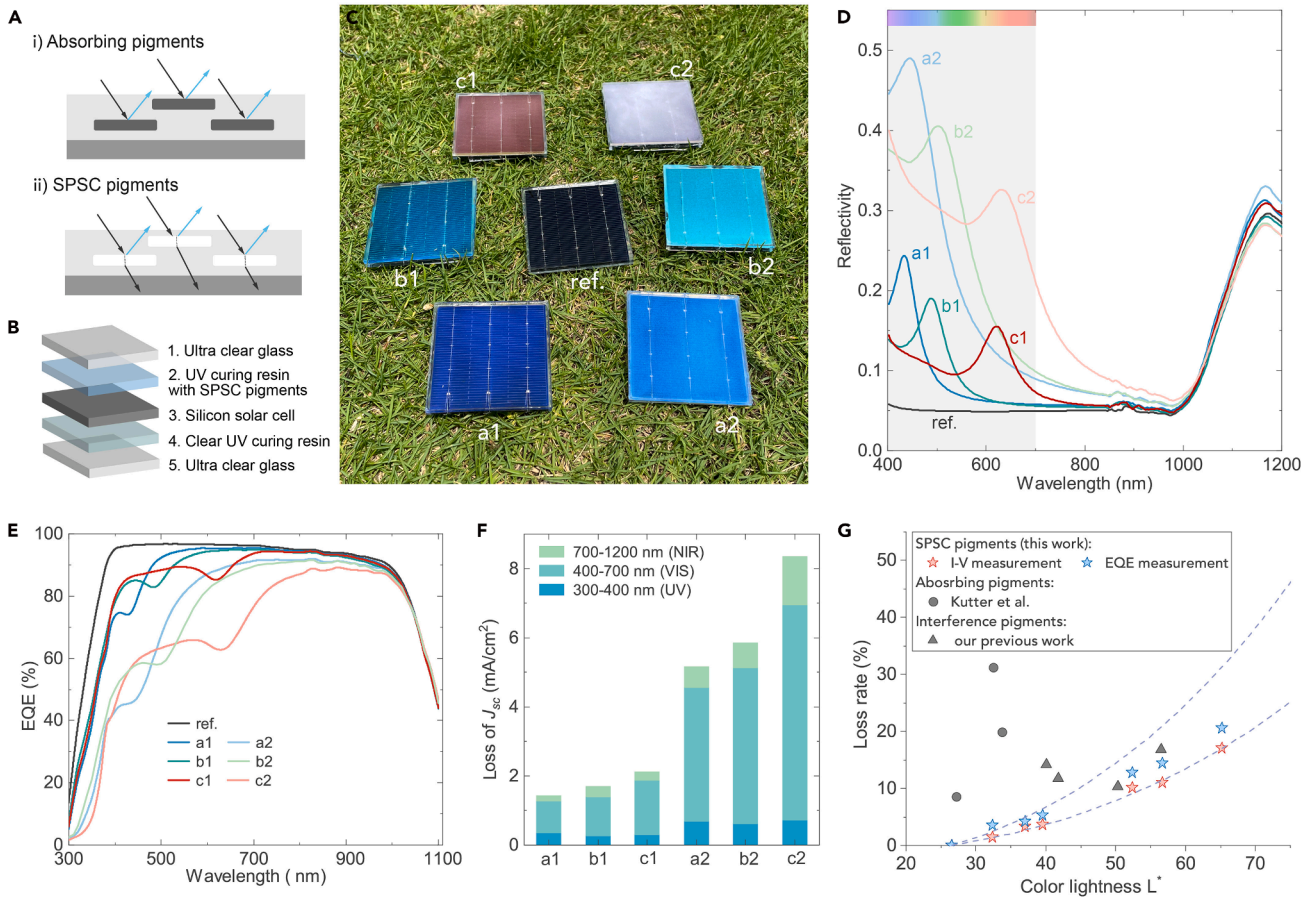

Figure 4. Colored PV modules enabled by SPSC pigments

(A) Illustration comparing the optical characteristics of absorbing pigments and structural color pigments.

(B) The structure and components of the small-sized PV modules.

(C) Photograph of the small-sized PV modules appearing in different colors (ref. nos. of pigments: a1, 174-ETPTA; a2, 174-OPPEA; b1, 195-ETPTA; b2, 195-OPPEA; c1, 247-ETPTA; c2, 247-OPPEA).

(D) Spectral reflectivity of those PV modules.

(E) Spectral EQE of those PV modules.

(F) Loss of short-circuit current density (J_{sc}) compared with the black PV module (ref.), divided into different wavelength range: UV light, visible (vis) light, and near-infrared (NIR) light. Calculated based on EQE data.

(G) Relative loss rate of J_{sc} compared with the reference black PV module. The data of colored PV modules using absorbing pigments are from Kutter et al.[49] and the dashed lines are determined by the method provided in Note S3.

silica and polyacrylates are inherently transparent for visible-to-NIR light, resulting in high transmittance (Figure S12). Therefore, when applying the pigments in a coloring coating, most of the incident light will be transmitted to substrates (Figure 4A). This makes them ideal for coloring PV modules. To demonstrate that, we have fabricated PV modules with 52 × 52 mm^2 silicon solar cells and double-glazed structures. UV-curable resins, made by dispersing the SPSC pigments in aliphatic polyurethane acrylates, were used as an adhesive layer to simultaneously encapsulate and color the underlying solar cell (Figure 4B and methods). Compared with the black PV module encapsulated by a clear resin (Figure 4C, ref.), the other PV modules display a range of colors enabled by different SPSC pigments (see also Figure S13). By using pigments composed of ETPTA, the PV modules (a1, b1, and c1) show vivid colors with moderate brightness and distinct reflection peaks in visible wavelengths (Figure 4D), while their spectral reflectivity at NIR wavelengths is only slightly increased. Displayed colors get noticeably brighter for the PV modules using pigments made of OPPEA (a2, b2, and c2), originating from their higher and broader reflection peaks. Note that sample c2 appears grayish-white and the solar cell is almost invisible. However, counter-intuitively, it still exhibits very low NIR reflection.

Because of the increase in reflectivity, the EQE for these colored PV modules inevitably declines, but as desired, such a decrease primarily occurs at visible wavelengths (Figure 4E). We calculated theoretical short-circuit current (J_{sc}) under standard AM1.5G solar illumination based on the EQE data. As presented in Figure 4F, the J_{sc} loss for samples a1, b1, and c1 is found to be within 2.1 mA/cm^2, representing a remarkably low loss rate within 5% compared with the black PV module. With brighter colors, samples a2, b2, and c2 exhibit slightly higher J_{sc} loss, but the majority (75%) still come from reflecting visible light. We further performed current-voltage measurements under standard test conditions (Figures S14 and S15). As results show, the open-circuit voltage (V_{oc}) and fill factor (*FF*) have negligible differences between different PV modules, and the loss of PCE is primarily governed by J_{sc} (Table S2). Compared with the reference black PV module with a PCE of 22.1%, samples a1, b1, and c1 show 1.9%–5.2% relative loss and have a PCE of approximately 21%. Notably, the brightly colored PV modules still demonstrate respectable PCE values of 19.6% (a2), 19.4% (b2), and 17.8% (c2), respectively.

The high PCE of colored PV modules originates from the low J_{sc} loss during the coloring process using SPSC pigments. The loss is close to the theoretical minimum achieved by selectively reflecting only visible light within 400–760 nm (the lower dashed line in Figure 4G; see also Note S3). In contrast, using traditional absorbing pigments leads to a significantly larger loss rate in J_{sc} and PCE, even up to 10 times larger.[32,36,49] Moreover, the rapid decline in reflectivity for NIR

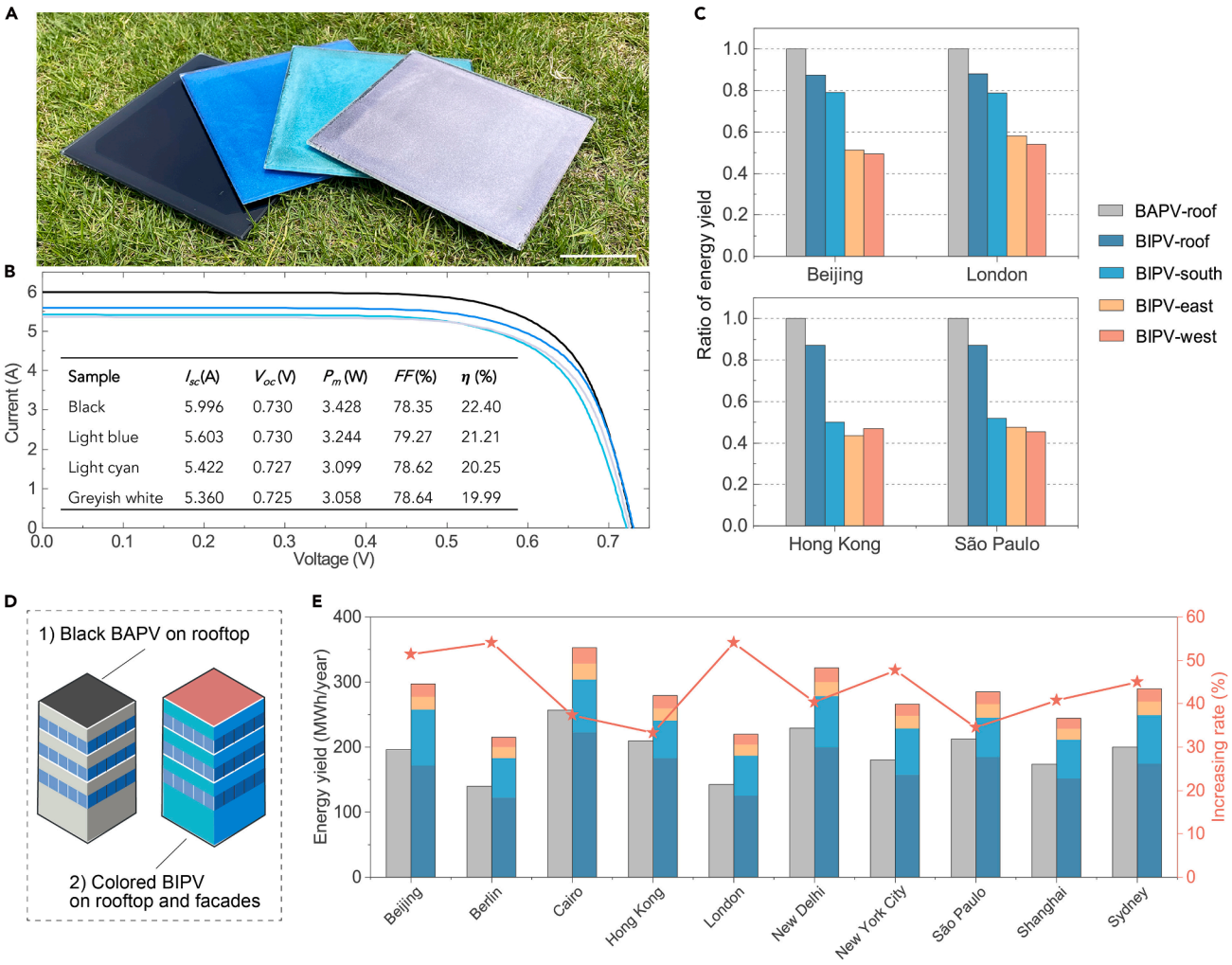

Figure 5. Potential for BIPV application

(A) Photograph showing the black, light blue, light cyan, and grayish-white PV modules, with the color originating from the SPSC pigments printed on the backside of glass covers. Scale bar, 5 cm.

(B) The current-voltage curves of the PV modules in (A). Inset: a table listing short-circuit current (I_{sc}), open-circuit voltage (V_{oc}), maximum power (P_m), fill factor (FF), and PCE (η).

(C) The yearly energy yield of a BAPV system on rooftops and colored BIPV systems on both rooftops and different facades, normalized over the value of the rooftop BAPV system.

(D) Illustration of two different building PV systems, as simulation cases.

(E) Comparison of the yearly energy yield for the two different building PV systems installed on a typical four-story midrise apartment building in 10 large cities all over the world.

light also enables lower J_{sc} loss compared with non-absorbing interference pigments. The resulting colored PV modules exhibit a remarkable enhancement of over 50% in PCE compared with modules employing traditional absorbing pigments, showcasing an even more vibrant color (Table S3). When compared with non-absorbing pigments such as white pigments and interference pigments, a notable improvement of 10%–30% is also observed. In the case of colored PV modules employing multilayered thin film coatings, those utilizing SPSC pigments achieve higher PCE levels than commercially available products,[17,50] and demonstrate comparable performance with those colored PV modules incorporating well-designed thin film stacks (Table S3).[20]

DISCUSSION

Potential for BIPV application

To demonstrate the potential for practical applications, we proceeded to manufacture colored PV modules employing a standard industrial process. This process involved laminating cover glass, ethylene vinyl acetate (EVA), solar cells, and a black backsheet together (Figure S16). The only additional step introduced was the application of SPSC pigments via printing on the inner side of the glass covers. Additionally, we utilized interdigitated back contact (IBC) solar cells that lack metal grids on the front side. Consequently, the PV modules depicted in Figure 5A look nothing like conventional ones, presenting a uniform and esthetically pleasing appearance. In comparison with the black module with a PCE of 22.40%, the light blue, light cyan, and grayish-white PV modules achieved PCEs of 21.21%, 20.25%, and 19.99%, respectively (Figure 5B; Table S4).

Based on these results, we believe that conventional PV modules can be transformed into visually appealing ones at an average relative PCE loss within 10%. In this regard, although a BIPV using such colored PV modules exhibits lower PCE and higher operating temperature, when deployed on a flat rooftop it can still generate over 87% of the annual energy yield of a rooftop building-adapted PV system (BAPV) (Figure 5C; Note S5). Besides, conventional black PV modules are mostly restricted on rooftops, while the potential of facades has not been well tapped due to higher esthetic demand. The esthetically

pleasing PV modules can promote BIPV deployment on facades, thus greatly increasing the building PV capacity to be installed. As the simulation results show (Figure 5C), the colored PV modules integrated with the south (or north) facades can provide nearly 79% energy yield in high-latitude regions such as Beijing and London. In low-latitude regions such as Hong Kong and São Paulo, it remains above 50%. Colored BIPV systems on east and west facades also have 40%–60% of power generation capacity (Figure S17; Table S5).

Further, we simulated the yearly energy yield of two different building PV systems as illustrated in Figure 5D, i.e., a black BAPV system on a rooftop and a colored BIPV system on both the rooftop and facades, in a typical four-story midrise apartment building (Figure S18; Note S5). We compared performance across 10 large cities worldwide to assess the potential benefits of widely employing colored BIPVs in different densely populated urban regions (Figure 5E). Thanks to the esthetically pleasing PV modules integrated with building facades, the energy yield of building PV systems can be significantly improved by over 50% in high-latitude regions and over 33% in low-latitude regions. If a high-rise building such as a ten-story apartment building is considered, the increasing rate of energy yield will be much larger, about 200% in most urban regions (Figure S19).

Further performance improvement

The primary objective of the colored PV samples presented in this work is to investigate the impact of SPSC pigments on the color appearance and I-V characteristics of PV modules, and to demonstrate their ease of integration in PV module colorization. As revealed by our theoretical analysis and confirmed by experimental results, applying a colored layer atop solar cells primarily reduces EQE and J_{sc} depending on the optical properties of colorants. Therefore, further enhancements in PCE can be easily realized through using solar cells with higher international quantum efficiency, V_{oc}, and FF. Notably, state-of-the-art commercial black c-Si PV modules have achieved PCEs ~26%.[51] Based on this, colored modules incorporating our photonic pigments are projected to reach PCEs above 23%. Further performance gains can be realized by using multijunction solar cells with higher theoretical efficiency limits—such as perovskite-silicon tandem cells.[52] Importantly, integrating such tandem cells into colored PV modules may offer a mutually beneficial strategy: the colorization can reduce the stringent bandgap requirements for the perovskite top cell, facilitating more stable[53] and esthetically versatile designs.

Further improvement of the coloring layer's optical properties remains an important objective. For instance, the SPSC pigments developed in this study result in a notable reduction in EQE within the UV range, owing to the strong UV scattering induced by their quasi-ordered photonic structures. Additionally, reducing reflectance in the NIR region could help mitigate further PCE losses. Nonetheless, we emphasize that achieving non-iridescent structural colors inevitably entails certain optical trade-offs, as isotropic light scattering is intrinsically more broadband. One promising strategy to address these limitations may involve the integration of downshifting photoluminescent materials, which absorb high-energy photons and re-emit in visible (vis) and NIR light.[54] Given that the current design already demonstrates favorable optical characteristics, including negligible parasitic absorption and low NIR reflection, the key challenge moving forward is not the pursuit of an ideal reflectance spectrum, but rather the optimization of practicality and cost-effectiveness for real-world deployment, as will be discussed in the following.

Toward practical implementation

It is recognized that the colored PV modules based on industrial-mature coloring technology, such as inorganic pigments and multilayer thin film coatings, have already been implemented in real buildings.[16,37] To further unlock the vast potential of colored PVs in integrated applications, new technologies must combine the strengths of existing approaches while avoiding their shortcomings—achieving natural coloration, high efficiency, and low cost simultaneously. This study demonstrates that the proposed bird-feather-inspired optical design successfully fulfills the first two criteria. As for the cost-effectiveness and manufacturing compatibility, we propose a solution based on pigmenting quasi-ordered photonic structural color materials. This approach offers excellent flexibility for integration into PV module fabrication: the pigments can be printed onto glass surfaces or incorporated directly into encapsulation polymers. Furthermore, paints containing these pigments can also be applied to already-installed PV modules for coloration, without requiring any complex processing steps.

To this end, materials innovation is of critical importance. The SPSC pigments proposed in this work are composed solely of two widely used, sustainable industrial materials—silica and polyacrylate—and are fabricated through scalable processes at regular environments. These features lay a solid foundation for their low-cost, large-scale application. Moving forward, refining the material design and manufacturing methods, as well as conducting field tests under practical environmental conditions, will be essential for advancing toward real-world implementation.

METHODS

Synthesis of monodisperse silica microspheres

All chemicals were purchased commercially and used as received. The monodispersed silica microspheres are synthesized by a two-step method. In a typical process, 5.5 mL tetraethyl orthosilicate (TEOS) was dissolved with 0.087 g of arginine in 87 mL of water and stirred at a constant temperature of 70°C for 24 h to obtain the silica seed solution. Next, 600 mL ethanol, 24 mL water, and 42 mL ammonia (28%), together with 0.7 mL seed solution, were mixed homogeneously. After that, 48 mL TEOS was slowly added dropwise to the solution, which was constantly stirred at 25°C. 12 h after, the final solution was centrifuged (4,000 rpm, 15 min) and the precipitate was dried at 70°C for 6 h to get the final products. The microsphere size was modified by changing the usage of the seed solution. In this study, the silica microspheres with diameters around 174, 195, and 247 nm were obtained by using 0.7, 0.5, and 0.23 mL seed solutions, respectively.

Preparation of SPSC pigments

The pigments were prepared using a process referred to as the C (centrifugation) I (infiltration) C (curing) G (grinding) method. In this study, the centrifugation process was completed in the final step of synthesizing silica microspheres. Then, the dried silica microspheres were infiltrated in a solution of acrylate monomer (such as ETPTA). Note the solution had added 1% photo-initiator 1173 (2-hydroxy-2-methyl-1-phenyl-1-propanone). Generally, several hours were enough for the silica microspheres to be completely infiltrated with acrylate monomer, and heating could be used to accelerate this process. Then, the additional acrylates were removed by suction filtration, which could be collected for recycling use. Immediately after, the silica microspheres were placed under an LED UV lamp (365 nm) for 10 s, causing the acrylate to be polymerized and forming the precursors of the SPSC pigments. Finally, these precursors were ground into powder by a rotary blade pulverizer. A 150-mesh screen was used to sort the pigment size.

Fabrication of colored PV modules

The small-sized PV modules in Figure 4C were made of five layers, i.e. (from top to bottom) a 2-mm-thick ultra-clear glass, UV curing resins with SPSC pigments, a 52 × 52 mm^2 silicon solar cell, clear UV curing resins, and a 2-mm-thick ultra-clear glass (Figure 4B). In detail, the glass has an average transmittance of nearly 92%; the colored resins were made by dispersing the pigments in aliphatic polyurethane acrylates diluted with an appropriate amount of isobornyl acrylate, together with 1 wt % photo-initiator 184 (1-hydroxycyclohexyl phenyl ketone) and 0.5 wt % organic silicon defoamer; the silicon solar cells were obtained by laser cutting from industrial-sized PERC solar cells, and they were soldered with tinned copper tapes on their busbars. The colored resins were blade coated onto the cover glass, and then a solar cell was placed on it and vacuumed to eliminate air bubbles. The resin was then cured under UV light to bond the solar cell to the glass. Subsequently, the backside of the solar cell was coated with

clear resins, followed by covering the backside glass and UV curing the resins.

The PV modules in Figure 5A were made of all industrial raw materials, including 3.2-mm-thick ultra-white tempered glasses, EVA adhesive films, IBC solar cells (SunPower Maxeon), and black backsheets. To make the colored and grayish-white PV modules, the glass was blade coated with the colored resins containing SPSC pigments, which were subsequently UV cured using a 365 nm LED UV light. The coated glass and the other materials were laminated together by a typical solar lamination machine to make the PV modules.

Characterization

A field emission SEM (Sigma 500, Zeiss) was used to observe the morphology of the silica microspheres and SPSC pigments, which were directly attached to the conductive adhesive and coated with Au. The SEM images were operated at an acceleration voltage of 5 kV and a working distance of 6.1 mm.

FTIR spectroscopy was performed on SPSC pigments, pure silica microspheres, and polymerized ETPTA, which were pressed tablets together with KBr. The samples were directly placed over the window of the spectrometer (Nicolet 6700, Thermo Fisher Scientific) to measure transmittance. Each spectrum results from 16 scans on one location of each sample.

TGA was performed using a simultaneous thermal analyzer (STA 449F3, Netzsch) within a nitrogen flow. The temperature range was 30°C–900°C with a heating rate of 10°C/min.

SAXS was measured by a Xeuss 3.0 UHR SAXS/WAXS beamline system (Xenocs). The sample was a 300-μm-thick film, which was made by dispersing the SPSC pigments (174-ETPTA) in a polyurethane acrylate (with 1 wt % photo-initiator 1173) and then UV curing it. The scattering data were collected using a Cu Kα radiation source with a wavelength of 1.54 Å, and an in-vacuum Eiger2 R 1M detector 4.6 m from the sample.

Optical micrographs were taken by a digital microscope (VHX-7000, Keyence) equipped with a fully integrated head lens (VHX-E20 and VHX-E100). Prior to imaging, the structural color pigments, either interference pigments or SPSC pigments, were spread out on a black plate, and some acrylate (ETPTA) was added dropwise to the plate to fully saturate the pigments. This would eliminate the broadband scattering from the silica microsphere-air interface. Before imaging it, the white balance was calibrated with white paper. During imaging, the structural color pigments were illuminated by circular lighting.

The spectral reflectivity and transmissivity of the PV glass covers, PV modules, and the color films made by SPSC pigments were characterized by using a UV-vis-NIR spectrophotometer (Lambda 950, PerkinElmer), which was equipped with a 150 mm diameter integrating sphere to measure the total reflection and transmission spectra at 8° incidence. A standard white diffuser was used as a reflectance standard. The exposure area of the samples was larger than 7 cm^2 and the data were collected with a 3 nm interval. Note that a part of busbars on silicon solar cells was also included in the measured region.

The EQE spectrum of PV modules in a wavelength range of 300–1,100 nm was measured using a QEX10 Solar Cell Quantum Efficiency Measurement System (PV Measurements), with a beam size of 1×5 mm and a 10 nm measurement interval. For each sample, three different positions on the surface were measured and then averaged as the result. The current-voltage characteristics of PV modules were measured using the Moduletest3 IV measurement system (h.a.l.m.). All measurements were conducted under standard test conditions (25°C, 1,000 W/m^2). During the measurement, the whole surface of PV modules was illuminated without using any mask. All the current-voltage curves were obtained in forward scan, with a sample time of about 40 ms. Note for the PV modules made by IBC solar cells, both forward scan and reverse scan were performed to eliminate capacitive effects on FF measurement.

RESOURCE AVAILABILITY

Lead contact

Further information and requests for resources should be directed to and will be fulfilled by the lead contact, Tao Ma (tao.ma@sjtu.edu.cn).

Materials availability

The photonic pigments generated in this study will be made available upon reasonable request.

Data and code availability

- This paper does not report the original code.
- All data are available in the main text and supplemental information.
- Additional data are available from the authors upon request.

ACKNOWLEDGMENTS

We thank Y. Yu, R. Iv, and B. Huang from Canadian Solar for the I-V measurement of PV modules. We appreciate Nano-X from Suzhou Institute of Nano-Tech and Nano-Bionics for the support in SAXS measurement. This work was financially supported by the National Natural Science Foundation of China (NSFC) through grant 52376201, the Science and Technology Commission of Shanghai Municipality through Grant 25DZ3002200, and the National Key R&D Program of China through grants 2022YFB4201003 and 2022YFB4200902.

AUTHOR CONTRIBUTIONS

Conceptualization, Z.L. and T.M.; investigation, Z.L., T.M., Y.C., and S.L.; methodology, Z.L. and T.M.; resources, T.M., Y.D., and D.Z.; funding acquisition, T.M.; supervision, T.M., Y.D., H.Y., and J.Y.; writing – original draft, Z.L., T.M., and S.L.; writing – review & editing, T.M., Y.D., H.Y., and J.Y.

DECLARATION OF INTERESTS

The authors declare no competing interests.

SUPPLEMENTAL INFORMATION

Supplemental information can be found online at https://doi.org/10.1016/j.ynexs.2025.100101.

Received: June 21, 2025
Revised: August 30, 2025
Accepted: August 31, 2025
Published: October 17, 2025

REFERENCES

1. Programme, U.E. (2025). Global Status Report for Buildings and Construction 2024/2025.
2. Lin, K., Chen, S., Zeng, Y., et al. (2023). Hierarchically structured passive radiative cooling ceramic with high solar reflectivity. Science 382, 691-697.
3. Li, J., Dong, K., Zhang, T., et al. (2023). Printable, emissivity-adaptive and albedo-optimized covering for year-round energy saving. Joule 7, 2552-2567.
4. Wang, S., Jiang, T., Meng, Y., et al. (2021). Scalable thermochromic smart windows with passive radiative cooling regulation. Science 374, 1501-1504.
5. Abraham, E., Cherpak, V., Senyuk, B., et al. (2023). Highly transparent silanized cellulose aerogels for boosting energy efficiency of glazing in buildings. Nat. Energy 8, 381-396.
6. Peng, Y., Fan, L., Jin, W., et al. (2021). Coloured low-emissivity films for building envelopes for year-round energy savings. Nat. Sustain. 5, 339-347.
7. Staffell, I., Pfenninger, S., and Johnson, N. (2023). A global model of hourly space heating and cooling demand at multiple spatial scales. Nat. Energy 8, 1328-1344.
8. Ballif, C., Perret-Aebi, L.-E., Lufkin, S., et al. (2018). Integrated thinking for photovoltaics in buildings. Nat. Energy 3, 438-442.
9. Virtuani, A., Borja Block, A., Wyrsch, N., et al. (2023). The carbon intensity of integrated photovoltaics. Joule 7, 2511-2536.
10. Faes, A., Virtuani, A., Quest, H., et al. (2025). Building-integrated photovoltaics. Nat. Rev. Clean Technol. 1, 333-350.

11. Hille, S.L., Curtius, H.C., and Wüstenhagen, R. (2018). Red is the new blue – The role of color, building integration and country-of-origin in homeowners' preferences for residential photovoltaics. Energy Build. 162, 21-31.

12. Awuku, S.A., Bennadji, A., Muhammad-Sukki, F., et al. (2021). Myth or gold? The power of aesthetics in the adoption of building integrated photovoltaics (BIPVs). Energy Nexus 4, 100021.

13. Halme, J., and Mäkinen, P. (2019). Theoretical efficiency limits of ideal coloured opaque photovoltaics. Energy Environ. Sci. 12, 1274-1285.

14. Li, Z., and Ma, T. (2022). Theoretic efficiency limit and design criteria of solar photovoltaics with high visual perceptibility. Appl. Energy 324, 119761.

15. Røyset, A., Kolås, T., and Jelle, B.P. (2020). Coloured building integrated photovoltaics: Influence on energy efficiency. Energy Build. 208, 109623.

16. Li, Z., Li, S., Yan, J., et al. (2025). Balancing aesthetics and efficiency of coloured opaque photovoltaics. Nat. Rev. Clean Technol. 1, 216-226.

17. Bläsi, B., Kroyer, T., Kuhn, T.E., et al. (2021). The MorphoColor Concept for Colored Photovoltaic Modules. IEEE J. Photovolt. 11, 1305-1311.

18. Ortiz Lizcano, J.C., Procel, P., Calcabrini, A., et al. (2022). Colored optic filters on c-Si IBC solar cells for building integrated photovoltaic applications. Prog. Photovolt. 30, 401-435.

19. Shafian, S., Eun Lee, G., Yu, H., et al. (2022). High-Efficiency Vivid Color CIGS Solar Cell Employing Nondestructive Structural Coloration. Sol. RRL 6, 2100965.

20. Xu, Z., Matsui, T., Matsubara, K., et al. (2022). Tunable and angle-insensitive structural coloring of solar cell modules for high performance building-integrated photovoltaic application. Sol. Energy Mater. Sol. Cell. 247, 111952.

21. Rudzikas, M., Donėlienė, J., Bužavaitė-Vertelienė, E., et al. (2023). Design and investigation of 1D photonic crystal based structures for BIPV cell colorization by sol-gel dipping technology. Sol. Energy 250, 285-294.

22. Manwani, K., Lagier, M., Krammer, A., et al. (2024). Development of novel orange colored photovoltaic modules with improved angular stability and high energy efficiency. Sol. Energy Mater. Sol. Cell. 278, 113144.

23. Peharz, G., Berger, K., Kubicek, B., et al. (2017). Application of plasmonic coloring for making building integrated PV modules comprising of green solar cells. Renew. Energy 109, 542-550.

24. Bae, S., Noh, Y.W., Park, D.-S., et al. (2022). Development of colored perovskite solar cells using cholesteric helicoidal superstructures. Nano Energy 93, 106801.

25. Jiang, C., Zhang, G., Hong, Z., et al. (2023). Colored Silicon Heterojunction Solar Cells Exceeding 23.5% Efficiency Enabled by Luminescent Down-Shift Quantum Dots. Adv. Mater. 35, 2208042.

26. Middleton, R., Tunstad, S.A., Knapp, A., et al. (2024). Self-assembled, disordered structural color from fruit wax bloom. Sci. Adv. 10, eadk4219.

27. Jeon, D.-J., Ji, S., Lee, E., et al. (2023). How the Eurasian Jay Expands its Color Palette by Optimizing Multiple Scattering. Adv. Opt. Mater. 11, 2202210.

28. Okazaki, T. (2020). Role of spongy layer and melanin granule arrangement on the development of blue structural color of bird feathers. Int. J. Anal. Bio-Sci. 8, 9-17.

29. Levinson, R., Berdahl, P., and Akbari, H. (2005). Solar spectral optical properties of pigments—Part II: survey of common colorants. Sol. Energy Mater. Sol. Cell. 89, 351-389.

30. Saretta, E., Frontini, F., Bonomo, P., et al. (2016). Indoor and outdoor characterization of innovative colored BIPV modules for facade application. In 32nd European Photovoltaic Solar Energy Conference and Exhibition.

31. Riedel, B., Messaoudi, P., Assoa, Y.B., et al. (2021). Color coated glazing for next generation BIPV: performance vs aesthetics. EPJ Photovolt. 12, 11.

32. Eggers, H., Gharibzadeh, S., Koch, S., et al. (2022). Perovskite Solar Cells with Vivid, Angle-Invariant, and Customizable Inkjet-Printed Colorization for Building-Integrated Photovoltaics. Sol. RRL 6, 2100897.

33. Wang, D., Liu, Z., Wang, H., et al. (2023). Structural color generation: from layered thin films to optical metasurfaces. Nanophotonics 12, 1019-1081.

34. Kim, J.B., Chae, C., Han, S.H., et al. (2021). Direct writing of customized structural-color graphics with colloidal photonic inks. Sci. Adv. 7, eabj8780.

35. Hwang, V., Stephenson, A.B., Barkley, S., et al. (2021). Designing angle-independent structural colors using Monte Carlo simulations of multiple scattering. Proc. Natl. Acad. Sci. USA 118, e2015551118.

36. Saw, M.H., Singh, J.P., Wang, Y., et al. (2020). Electrical Performance Study of Colored c-Si Building-Integrated PV Modules. IEEE J. Photovolt. 10, 1027-1034.

37. Borja Block, A., Escarre Palou, J., Courtant, M., et al. (2024). Colouring solutions for building integrated photovoltaic modules: A review. Energy Build. 314, 114253.

38. Eder, G., Peharz, G., Trattnig, R., et al (2019). Coloured BIPV Market, Research and Development IEA PVPS Task 15, Report IEA-PVPS T15-07: 2019.

39. Wang, Z., Chan, C.L.C., Haataja, J.S., et al. (2022). Deconvoluting the Optical Response of Biocompatible Photonic Pigments. Angew. Chem. Weinheim. Bergstr. Ger. 134, e202206562.

40. Park, J.-G., Kim, S.-H., Magkiriadou, S., et al. (2014). Full-Spectrum Photonic Pigments with Non-iridescent Structural Colors through Colloidal Assembly. Angew. Chem. Int. Ed. 53, 2899-2903.

41. Clough, J.M., Guimard, E., Rivet, C., et al. (2019). Photonic Paints: Structural Pigments Combined with Water-Based Polymeric Film-Formers for Structurally Colored Coatings. Adv. Opt. Mater. 7, 1900218.

42. Cai, Z., Li, Z., Ravaine, S., et al. (2021). From colloidal particles to photonic crystals: advances in self-assembly and their emerging applications. Chem. Soc. Rev. 50, 5898-5951.

43. Bauernfeind, V., Djeghdi, K., Gunkel, I., et al. (2023). Photonic Amorphous I-WP-Like Networks Create Angle-Independent Colors in Sternotomis virescens Longhorn Beetles. Adv. Funct. Mater. 34, 2302720.

44. Demirörs, A.F., Poloni, E., Chiesa, M., et al. (2022). Three-dimensional printing of photonic colloidal glasses into objects with isotropic structural color. Nat. Commun. 13, 4397.

45. Saranathan, V., Forster, J.D., Noh, H., et al. (2012). Structure and optical function of amorphous photonic nanostructures from avian feather barbs: a comparative small angle X-ray scattering (SAXS) analysis of 230 bird species. J. R. Soc. Interface 9, 2563-2580.

46. Shi, L., Zhang, Y., Dong, B., et al. (2013). Amorphous Photonic Crystals with Only Short-Range Order. Adv. Mater. 25, 5314-5320.

47. Li, Z., Li, S., and Ma, T. (2023). Using Photonic Glasses as Colored Covers for Solar Energy Harvesting. Adv. Opt. Mater. 11, 2202370.

48. Jacucci, G., Vignolini, S., and Schertel, L. (2020). The limitations of extending nature's color palette in correlated, disordered systems. Proc. Natl. Acad. Sci. USA 117, 23345-23349.

49. Kutter, C., Bläsi, B., Wilson, H.R., et al. (2018). Decorated building-integrated photovoltaic modules: Power loss, color appearance and cost analysis. In 35th European PV Solar Energy Conference and Exhibition.

50. Jolissaint, N., Hanbali, R., Hadorn, J.-C., et al. (2017). Colored solar façades for buildings. Energy Proc. 122, 175-180.

51. Green, M.A., Dunlop, E.D., Yoshita, M., et al. (2025). Solar Cell Efficiency Tables (Version 66). Prog. Photovolt. 33, 795-810.

52. Pearce, P.M., Halme, J., Jiang, J.Y., et al. (2024). Efficiency limits and design principles for multi-junction coloured photovoltaics. Energy Environ. Sci. 17, 1189-1201.

53. Duan, L., Walter, D., Chang, N., et al. (2023). Stability challenges for the commercialization of perovskite–silicon tandem solar cells. Nat. Rev. Mater. 8, 261-281.

54. Sun, Z., Xia, Z., Yan, D., et al. (2025). Industrial-Scale Silicon Heterojunction Photovoltaic Module Towards 25% Efficiency Enabled by High-Quantum-Yield CaSrSiO4:Ce3+ Inorganic Downshifting Materials. Prog. Photovolt. 33, 678-688.